SUPPLEMENTAL FILE 1

Overproduction of the AlgT sigma factor is lethal to mucoid *Pseudomonas aeruginosa*

Ashley R. Cross, Vishnu Raghuram, Zihuan Wang, Debayan Dey,

and Joanna B. Goldberg

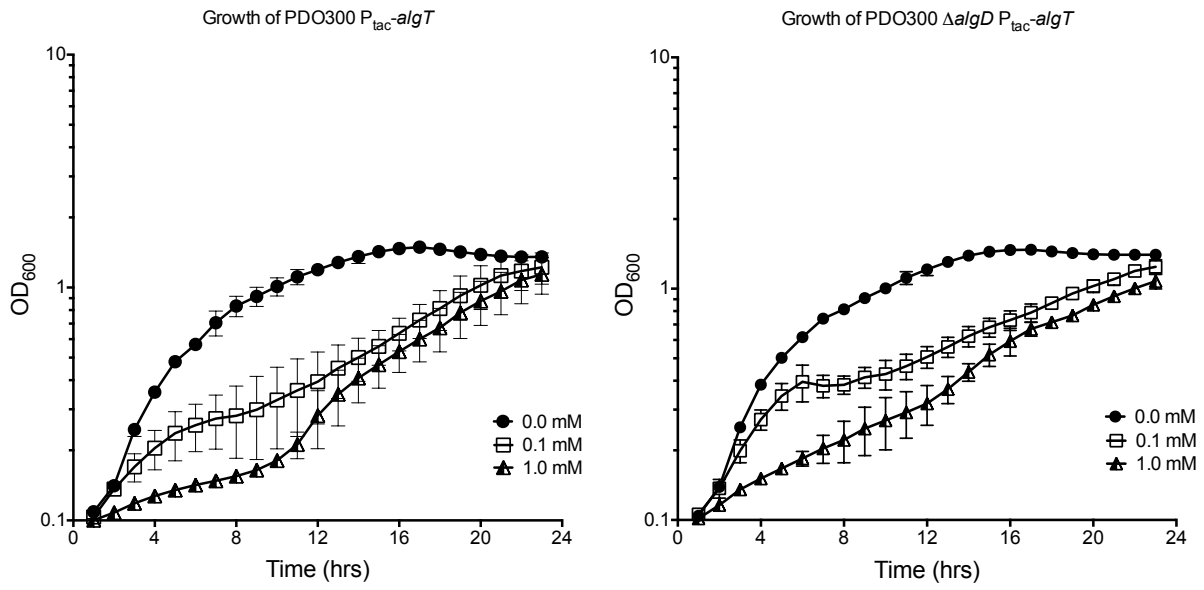

Figure S1. Overexpression of *algT* in PDO300 and PDO300 Δ*algD* reduces growth. Growth curves of each strain grown in LB containing no inducer, 0.1 mM IPTG, or 1.0 mM IPTG. The strains shown are PAC539 and PAC543.

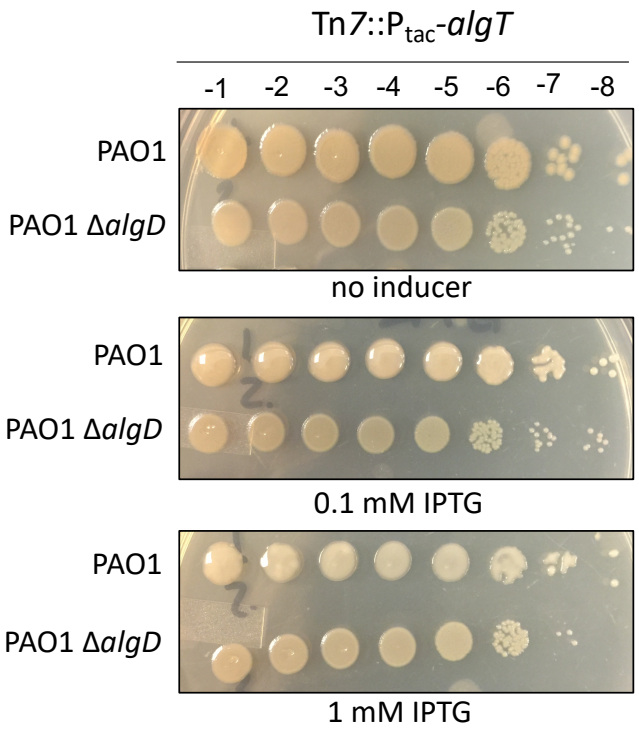

Figure S2. Overexpression of *algT* in strains containing wild type MucA is not lethal. The *algT* coding sequence was cloned downstream of an IPTG inducible tac promoter and inserted, in single copy, at the *att*Tn*7* site of each strain (Tn*7*::P_{tac}-*algT*). Overnight cultures were grown without inducer, normalized to an optical density of 0.5, and then serially diluted onto LA containing no inducer, 0.1 mM IPTG, and 1 mM IPTG. IPTG induces expression of *algT*. Corresponding dilutions factors are shown on top. PAO1 becomes mucoid when *algT* is expressed. The strains shown are PAC501 and PAC541.

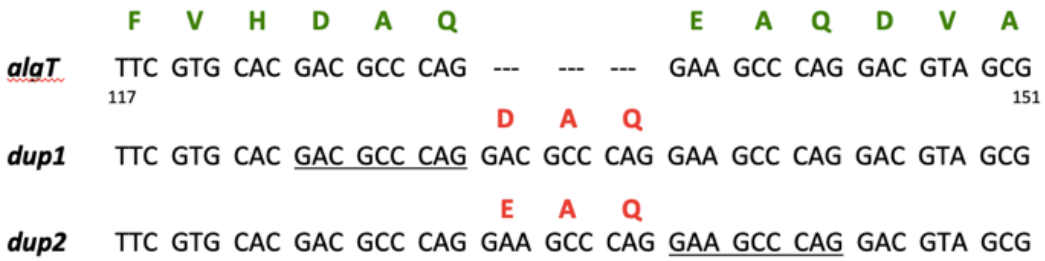

Figure S3. AlgT sequence alignment of two nonmucoid revertants. The AlgT amino acid sequence (green) is shown above the 117-151 bp nucleotide sequence (black). Both nonmucoid revertants had an in-frame duplication resulting in the insertion of three amino acids (red); DAQ (dup1) and EAQ (dup2). The underlined text represents the duplicated nucleotides.

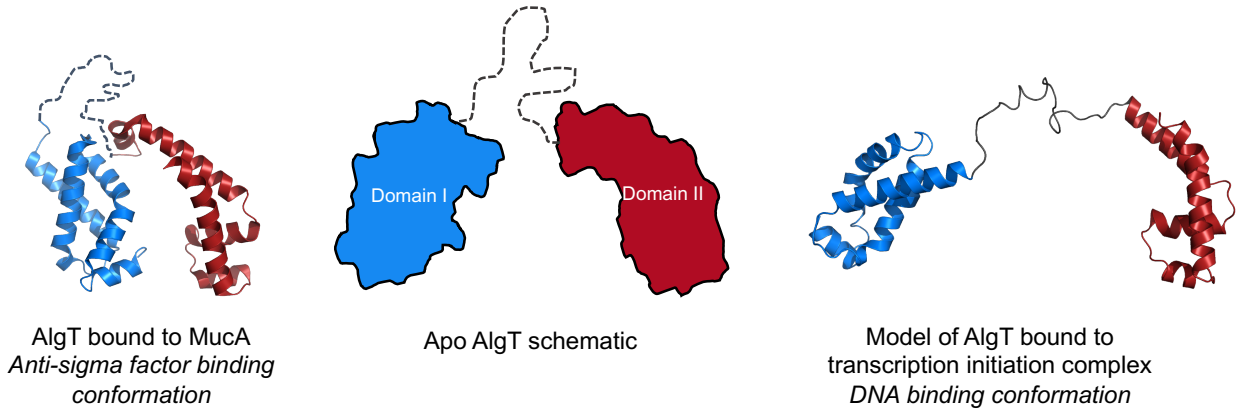

Figure S4. Structural models of *Pseudomonas* AlgT. The AlgT sigma factor is composed of two helical bundles which form the N-terminal domain I (blue) and C-terminal domain II (red) connected by a flexible 25 residue linker. The apo structure schematic is shown in the middle. Anti-sigma factor MucA binds AlgT and prevents it from binding to the RNA polymerase for transcription. The conformation of AlgT bound to MucA (PDB 6IN7) is shown in left, where domains I and II are arranged in a closed conformation. In contrast, AlgT interacts with the DNA in the transcription initiation complex with an extended linker conformation (right; modeled from RpoE-DNA complex, PDB 6JBQ), where domain I (in blue) engages the -10 element of the promoter and takes part in promoter melting, while the domain II (in red) interacts with -35 element of the promoter.

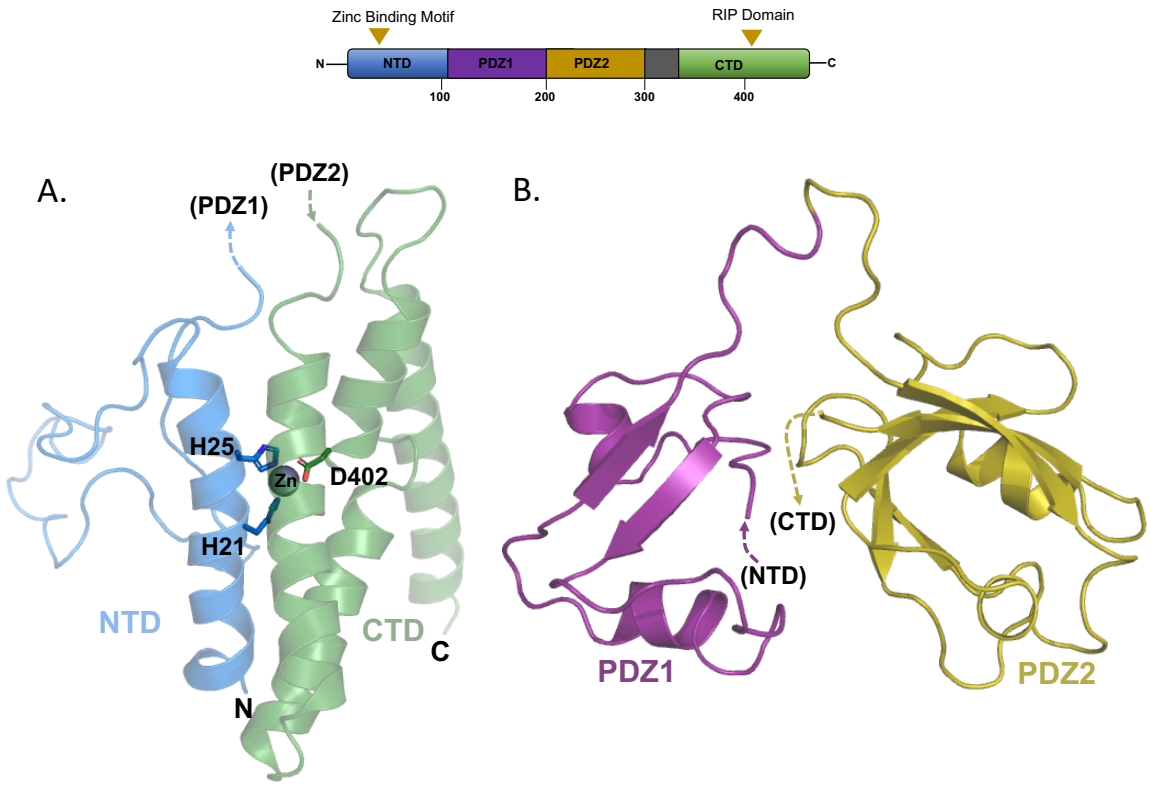

Figure S5. Homology model of MucP membrane bound and periplasmic domains. A) Model of membrane bound M50 peptidase domain of MucP modeled using *de novo* modeling using evolutionary and structural constrains with PDB 3B4R. As MucP does not share overall sequence similarity to any protein for which a structure has been determined, this model was generated *de novo* using structural constrains of the active site, helical constrains, secondary structure prediction, and using a distant homolog of MucP from *M. jannaschii*. B) Homology model of the two PDZ domains in MucP modeled with PDB 2FNE. PDZ1 is connected to the membrane bound N-terminal domain (NTD) while PDZ2 is connected to the membrane bound C-terminal domain (CTD). The catalytic core is composed of the NTD (His 21 and His 25), the CTD (D402), and a zinc metal cation.

Table S1. Genes identified with mutations in suppressors.

Strain	Gene Locus	Nucleotide Mutation	Location (total)	Product
PDO300 suppressor 1	PA4059	C insertion, frameshift	315(378)	hypothetical protein
PDO300 suppressor 2	PA4059	C insertion, frameshift	315(378)	hypothetical protein
PDO300 suppressor 3	PA3649	G insertion, frameshift	358(1353)	MucP, MucA protease
	PA4059	C insertion, frameshift	315(378)	hypothetical protein
PDO300 ΔalgD suppressor 1	PA3541	A1G, start codon variant	1(1485)	Alg8, alginate biosynthesis
	PA3649	CCCCCGC deletion, frameshift	910_916(1353)	MucP, MucA protease
	PA4059	C insertion, frameshift	315(378)	hypothetical protein
PDO300 ΔalgD suppressor 2	PA3541	A1G, start codon variant	1(1485)	Alg8, alginate biosynthesis
	PA4059	C insertion, frameshift	315(378)	hypothetical protein
PDO300 ΔalgD suppressor 3	PA3541	A1G, start codon variant	1(1485)	Alg8, alginate biosynthesis
	PA3649	TTATGGAGTCGAGCG deletion, in frame	1022_1036(1353)	MucP, MucA protease
	PA4059	C insertion, frameshift	315(378)	hypothetical protein
	PA4938	G462A, synonymous	462(1293)	PurA, adenylosuccinate synthetase

Table S2. Strains, plasmids, and primers used in this study.

Strains	Genotype or relevant features	Source
E. coli		
DH5α	cloning background, plasmid maintenance	Invitrogen
P. aeruginosa		
PAO1	wild type (nonmucoid)	1
PDO300	PAO1 *mucA22* (mucoid)	2
PAC342	PAO1 Δ*algD*	3
PAC437	PDO300 Δ*algD*	This study
PAC541	PAO1 CTX::P5$_{algT}$-optRBS-*lacZ* Tn*7*::P$_{tac}$-*algT*	This study
PAC501	PAC342 CTX::P5$_{algT}$-optRBS-*lacZ* Tn*7*::P$_{tac}$-*algT*	This study
PAC539	PDO300 CTX::P5$_{algT}$-optRBS-*lacZ* Tn*7*::P$_{tac}$-*algT*	This study
PAC543	PAC437 CTX::P5$_{algT}$-optRBS-*lacZ* Tn*7*::P$_{tac}$-*algT*	This study
PAC559	PAC539 pHERD20T-*mucA*	This study
PAC561	PAC543 pHERD20T-*mucA*	This study
PAC667	PAC577 pHERD20T-*mucP*	This study
PAC678	PAC579 pHERD20T-*mucP*	This study
PAC577	PAC539 suppressor (*mucP* 358 C insertion)	This study
PAC578	PAC539 suppressor (*algT* duplication 136-144 GAAGCCCAG)	This study
PAC579	PAC543 suppressor (*mucP* deletion 910-916 GCGGGGG)	This study
PAC581	PAC543 suppressor (*algT* C400T)	This study
PAC582	PAC543 suppressor (*mucP* deletion 1022-1036 CGCTCGACTCCATAA)	This study
Plasmids	**Description**	**Source**
miniTn*7*-P$_{tac}$-*algT*	IPTG inducible *algT* in single copy	4
pHERD20T	arabinose-inducible multicopy plasmid	5
pHERD20T-*mucA*	arabinose inducible *mucA* with an N-terminus HA tag	6
pHERD20T-*mucP*	arabinose inducible *mucP*, multicopy	This study
pEXG2-*mucA22*	*mucA22* allelic replacement vector	4
miniCTX-optRBS-*lacZ*	promoterless-*lacZ* reporter with optimized RBS, single-copy	4
miniCTX-P5$_{algT}$-optRBS-*lacZ*	*algT* promoter-*lacZ* reporter	This study

Primers	Sequence	Source
oAC32	GACCCACTCTCAGGAGTGAAC	4
oAC33	CTCTTCGCTATTACGCCAGCTG	4
oAC039	ATCGCAACTCTCTACTGTTTCT	5
oAC040	TGCAAGGCGATTAAGTTGGGT	5
oAC089	TTCCACACATTATACGAGCCGGAAGCATAAAT GTAAAGCAatgagtcgtgaagccctgca	4
oAC090	CGAGCTCGAGCCCGGGGATCCTCTAGAGTCGA CCTGCAGAtcagcggttttccaggctgg	4
oAC107	TGAGCCCGATGCAATCCAT	This study
oAC108	CAACTGGTAACGCGACCAG	This study
oAC158	CTGGAGCTCCACCGCGGTGGCGGCCGCTCTAG AACTAGTGatgcgcaggtgttccggaag	This study
oAC159	AATCATGGTCATAGCTGTTCCTCCTTACTGCAG CCCGGGGggaggagcttcgagcgtccc	This study
oAC276	GGTACCCGGGGATCCTCTAGAGTCGACCTGCA GGCATGCAatgagtgcgctttacatgat	This study
oAC277	TTTTCCCAGTCACGACGTTGTAAAACGACGGC CAGTGCCActacagacgactcagatcgt	This study

*lowercase nucleotides anneal to plasmid sequence during isothermal assembly

REFERENCES

1. Hancock REW, Carey AM. 1979. Outer membrane of *Pseudomonas aeruginosa*: heat- and 2-mercaptoethanol-modifiable proteins. J Bacteriol 140:902-910.
2. Mathee K, Ciofu O, Sternbrg C, Lindum PW, Campbell JIA, Jensen P, Johnsten AH, Givskov M, Ohman DE, Molin S, Hoiby N, Kharazmi A. 1999. Mucoid conversion of *Pseudomonas aeruginosa* by hydrogen peroxide: a mechanism for virulence activation in the cystic fibrosis lung. Microbiology 145:1349-1357.
3. Tseng BS, Zhang W, Harrison JJ, Quach TP, Song JL, Penterman J, Singh PK, Chopp DL, Packman AI, Parsek MR. 2013. The extracellular matrix protects *Pseudomonas aeruginosa* biofilms by limiting the penetration of tobramycin. Environ Microbiol 15:2865-78.
4. Cross AR, Goldberg JB. 2019. Remodeling of O antigen in mucoid *Pseudomonas aeruginosa* via transcriptional repression of *wzz2*. mBio 10:e02914-18.
5. Qiu D, Damron FH, Mima T, Schweizer HP, Yu HD. 2008. P_{BAD}-based shuttle vectors for functional analysis of toxic and highly regulated genes in *Pseudomonas* and *Burkholderia* spp. and other bacteria. Appl Environ Microbiol 74:7422-6.
6. Damron FH, Qiu D, Yu HD. 2009. The *Pseudomonas aeruginosa* sensor kinase KinB negatively controls alginate production through AlgW-dependent MucA proteolysis. J Bacteriol 191:2285-95.